American Mineralogist, Volume 81, pages 676–684, 1996

Experimental reversals of chlorite compositions in divariant $MgO + Al_2O_3 + SiO_2 + H_2O$ assemblages

JUDY BAKER AND T.J.B. HOLLAND

Department of Earth Sciences, University of Cambridge, Cambridge CB2 3EQ, U.K.

ABSTRACT

The compositions of chlorite in divariant assemblages involving orthopyroxene + forsterite and spinel + corundum were reversed at a range of temperatures for $P = 14$ kbar and a range of pressures for $T = 800$ °C. These compositions, determined using a new calibration of the variation in the c unit-cell parameter with X_{chl}, were then compared with those calculated using several simple activity-composition models for charge-balanced Tschermak substitutions in MASH chlorite. The discrepancies between the observations and calculations suggest that entropies of mixing are very low in chlorite solid solutions.

INTRODUCTION

Chlorite is a common mineral constituent of calc-silicate, pelite, mafic, and ultramafic bulk compositions and is stable over a range of low- to medium-grade pressure-temperature conditions. Within many of these bulk compositions, chlorite compositions are close to clinochlore [$Mg_5AlSi_3AlO_{10}(OH)_8$], with some compositional variation along $FeMg_{-1}$ and $Mg_{-1}Si_{-1}AlAl$ (Tschermak) solid solutions. An understanding of the thermodynamics of these compositional variations is thus an important tool in detailed studies of the P-T conditions of formation of low- to medium-grade metamorphic rocks.

The most accurate thermodynamic data for many mineral end-members are obtained from experimental reversals of univariant reactions. In the case of MgO-Al_2O_3-SiO_2-H_2O (MASH) chlorite, this approach is not straightforward because clinochlore is not an end-member mineral phase but lies in the middle of a solid solution between $Mg_6Si_4O_{10}(OH)_8$ and $Mg_4Al_4Si_2O_{10}(OH)_8$ (amesite). The general formula of MASH chlorite can thus be written $(Mg_{6-X}Al_X)(Si_{4-X}Al_X)O_{10}(OH)_8$, where $X = X_{chl}$, a measure of the Tschermak solid solution, varies from 0 to 2. The composition of chlorite should thus change by means of Tschermak substitution along any MASH univariant reaction, and, unless the composition of the chlorite is reversed at P-T points along each univariant reaction, extraction of thermodynamic data from experimental brackets requires some assumption about changes in chlorite composition with changing P and T; i.e., the activity-composition (a-X) relationship.

The 14 Å chlorite structure consists of alternating 2:1 talc-like and brucite-like sheets. There are four (two distinct) tetrahedrally coordinated sites in the 2:1 sheet, i.e., two T1 and two T2 sites; and six (four distinct) octahedrally coordinated sites, i.e., one M1 and two M2 sites in the 2:1 sheet, and two M3 and one M4 site in the brucite sheet. The distribution of the atoms among these sites is not well known, but there is a growing body of evidence (summarized in Welch et al. 1995) to suggest that both the tetrahedral and octahedral cations in chlorite are partially ordered. Although X-ray and neutron diffraction data for natural chlorite suggest that the tetrahedral cations are highly disordered, ^{29}Si magic-angle-spinning (MAS) NMR studies of other sheet silicates suggest considerable degrees of short-range order with Al avoidance. In addition, diffraction studies suggest that $^{[6]}Al$ is highly ordered on the M4 sites. On the basis of these observations, Holland and Powell (1990) derived thermodynamic data for the chlorite solid solution using a simple mixing model in which Al and Si were assumed to mix ideally on only two of the four tetrahedral sites (T2, labeled "t2" in their expressions) and, additionally, Al was assumed to mix ideally on only two of the six octahedral sites (M1 + M4, labeled "m2" in their expressions). Using the definition of X_{chl} from above, the activities of clinochlore ($X_{chl} = 1$) and amesite ($X_{chl} = 2$) in this model are then given by $a_{clin} = X^2(2 - X)^2$ and $a_{ames} = X^4/16$. Holland and Powell used this model, together with the experimental value of $X_{chl} = 1.2$ at 14 kbar and 860 °C as the conditions of the breakdown of chlorite to orthopyroxene + forsterite + spinel + H_2O (Jenkins 1981) to derive thermodynamic data for the amesite end-member.

Figure 1a shows the stability of reactions involving chlorite in the MgO-Al_2O_3-SiO_2-H_2O system across P-T space calculated using the Holland and Powell thermodynamic dataset (generated January 26, 1995) and the program THERMOCALC (Powell and Holland 1988, version 2.4). The calculated chlorite breakdown curve shown in Figure 1a passes through the experimentally determined brackets of Fawcett and Yoder (1966), Staudigel and Schreyer (1977), and Jenkins (1981). The simple a-X relationship of Holland and Powell (1990) is thus consistent with these experimental brackets. Figure 1b shows the calculated compositions of the chlorite along these univariant reactions. The chlorite along the chlorite

0003–004X/96/0506–0676$05.00

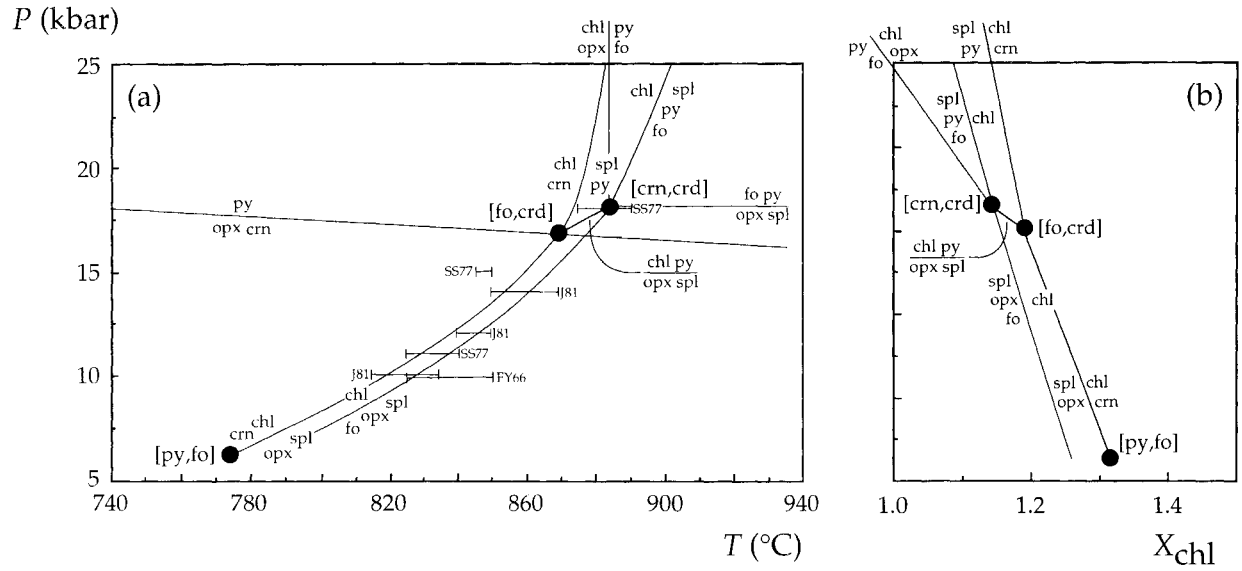

FIGURE 1. (**a**) *P-T* positions of the cordierite-absent univariant reactions in the system MgO-Al_2O_3-SiO_2-H_2O, calculated from the thermodynamic dataset of Holland and Powell (generated January 26, 1995) and the program THERMOCALC (Powell and Holland 1988, version 2.4) and assuming ideal mixing of Tschermak solid solution in the chlorite. Phases include chlorite (chl), corundum (crn), forsterite (fo), spinel (spl), pyrope (py), cordierite (crd), and orthopyroxene (opx). The positions of experimental reversals of the chlorite breakdown reaction to spinel + forsterite + orthopyroxene are shown for reference [FY66 = Fawcett and Yoder (1966), SS77 = Staudigel and Schreyer (1977), and J81 = Jenkins (1981)]. (**b**) Calculated compositions of chlorite along each of the univariant reactions in **a**. X_{chl} is defined in the text.

breakdown reaction shows a continuous change from more aluminous to less aluminous with increasing pressure (from X_{chl} = 1.26 at P = 5 kbar to X_{chl} = 1.1 at P = 25 kbar). However, the change in composition is small, and Chernosky et al. (1988) and Berman (1988) were able to fit these experimental brackets for chlorite breakdown using a fixed composition of chlorite, illustrating that univariant reactions do not place particularly narrow constraints on *a-X* relationships in chlorite solid solutions.

Jenkins and Chernosky (1986) presented experimental data on the compositions of Mg-Al chlorite coexisting with three divariant assemblages involving cordierite, orthopyroxene, and forsterite at P = 3 kbar. The chlorite compositions, unreversed in all cases, show significant changes with changing temperature. However, the calculated compositions of MASH chlorite in these divariant assemblages (Fig. 2b) derived using the Holland and Powell dataset and the simple *a-X* model do not pass through the experimental data points. This discrepancy suggests that the simple model is inappropriate for MASH chlorite and that reversals of chlorite compositions in divariant assemblages would provide a sensitive test of any proposed activity-composition relationships.

Figure 3 shows the compositional variation of chlorite in divariant assemblages at constant P = 14 kbar (Fig. 3a) and constant T = 800 °C (Fig. 3b) calculated using the Holland and Powell dataset and *a-X* model for chlorite. These diagrams illustrate that the composition of chlorite in some divariant assemblages deviates significantly from clinochlore; these deviations are large at lower temperatures and higher pressures, with the compositions converging on X_{chl} = 1.2 as the conditions of a univariant reaction is approached. In particular, these calculations predict that chlorite coexisting with corundum and spinel is significantly more aluminous than X_{chl} = 1.2 at conditions below the chlorite breakdown reaction, whereas, at the same conditions, chlorite coexisting with forsterite and orthopyroxene is significantly less aluminous than X_{chl} = 1.2. The purpose of this study is thus to reverse experimentally the composition of chlorite in these two divariant assemblages as a function of P and T and to use these compositions to determine the degree of nonideality in chlorite along the Tschermak solid-solution vector.

EXPERIMENTAL TECHNIQUES

Apparatus

Synthesis and reversal experiments were performed in three types of apparatus. Low-pressure (3 kbar) syntheses were performed in cold-seal vessels. Individual syntheses comprised 150 mg of oxide mix, which was sealed into a 20 mm long by 5 mm diameter gold capsule. Chlorite syntheses at these conditions also contained 50 mg of deionized water. The capsules were positioned in the cold-seal vessel using an alumina filling rod to minimize temperature gradients. Pressure was measured using

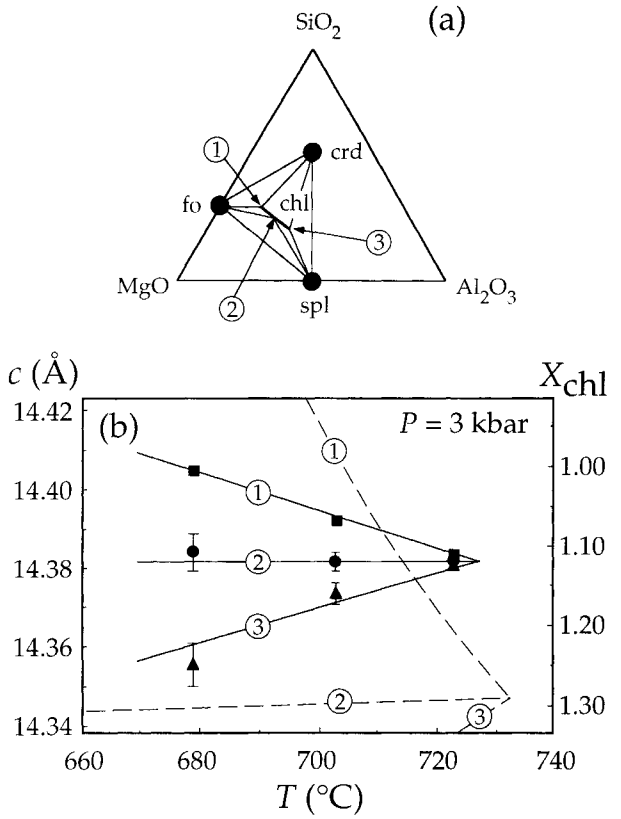

FIGURE 2. (a) A schematic MgO-Al_2O_3-SiO_2 compatibility triangle showing the stable tie lines between chlorite, cordierite, forsterite, and spinel at $P = 3$ kbar. Mineral abbreviations as in Figure 1. The composition of chlorite coexisting with cordierite + forsterite (1), forsterite + spinel (2), and cordierite + spinel (3) changes with temperature as shown in **b**. (b) A T-X_{chl}-c diagram drawn for $P = 3$ kbar comparing calculated and experimentally determined compositions of chlorite coexisting with cordierite + forsterite (1), forsterite + spinel (2), and cordierite + spinel (3) assemblages. The c-X_{chl} calibration used is that of Jenkins and Chernosky (1986). The squares, circles, and triangles show experimentally determined chlorite compositions from Jenkins and Chernosky (1986), and the dashed lines show the chlorite compositions calculated using the simple mixing model of Holland and Powell (1990).

a factory-calibrated gauge open to the vessel throughout the experiment, and pressures are accurate to ±50 bars. Temperature was measured with a calibrated, sheathed chromel-alumel thermocouple and is accurate to ±5 °C. The synthesis experiment at 7.1 kbar was made in an internally heated gas vessel (argon pressure medium) at the University of Edinburgh. Pressures were calibrated using the freezing point of mercury at 298 K, and the quoted pressure is accurate to ±20 bars. Pressure was recorded by a Manganin gauge open to the vessel throughout the experiment. Temperature was calibrated at 8 kbar using NaCl melting and is accurate to ±5 °C. The temperature gradient along the synthesis capsule was measured at ±6 °C. Syntheses at pressures of 14–15 kbar and all reversal experiments were performed in a piston-cylinder apparatus using a 0.75 in. NaCl assembly. Individual syntheses comprised 60 mg of oxide mix and 20 mg of deionized water, which were sealed into a 12 mm long by 5 mm diameter gold capsule. All experiments were performed under "piston-out" conditions (Danckwerth and Newton 1978); experiments were brought to pressures not <3.5 kbar below the desired experimental pressure and then heated to the desired temperature. Temperature was controlled using a chromel-alumel thermocouple and is accurate to ±5 °C. Pressure was continuously monitored during the experiment and controlled to ±0.1 kbar. Pressures in this piston-cylinder apparatus were calibrated at 16 kbar against a gas-apparatus determination of the equilibrium jadeite + quartz = albite (Hays and Bell 1973); for the set-up used, no pressure correction was necessary.

Starting materials

Chlorite samples a and b and an aluminous orthopyroxene (with 6 wt% Al_2O_3, the approximate composition of orthopyroxene coexisting with forsterite and spinel; Gasparik and Newton 1984) were synthesized from gel after the method of Hamilton and Henderson (1968). The gels were prepared by M.D. Welch using Mg metal (Aldrich no. PV05407TT), Al metal (Aldrich no. 59267), and tetraethyl orthosilicate (BDH lot no. 2124700). All other phases were synthesized from oxide mixes of MgO (Fisons AR lot no. 31728432), SiO_2 (Aldrich, 99.99% pure), and γ-Al_2O_3, prepared by firing $AlCl_3 \cdot 6H_2O$ (BDH lot no. 232B401563) at 400 °C for 1 h, 700 °C for 5 h, and 900 °C for 9 h. The compositions and synthesis conditions of the phases used in this study are given in Table 1.

After synthesis, all phases were examined optically, with X-ray diffraction, and finally with SEM to check for purity. The synthetic chlorite samples all comprised aggregates of fine-grained (5–30 μm) platy minerals with an X-ray diffraction pattern corresponding to the IIb-layer polytype (Brown and Bailey 1962). Small amounts (<5%) of spinel + corundum were observed in the products of one of the syntheses of chlorite a (no. 55), and 10–20% forsterite + orthopyroxene was observed in the products of synthetic chlorite c. Unit-cell parameters for all synthetic phases were determined with a HUBER Guinier Camera using Cu$K\alpha_1$ radiation and an internal elemental Si standard. Peak positions were calibrated by fitting a second-order polynomial to six silicon peaks (111, 220, 311, 400, 331, and 422). Unit-cell refinements were performed with the least-squares program CELL of Holland and Redfern (in preparation). Lattice parameters for the chlorite samples are discussed below; lattice parameters for the other synthetic phases are as follows: aluminous orthopyroxene, $a = 18.204(2)$, $b = 8.768(2)$, and $c = 5.174(1)$ Å; corundum, $a = 4.758(1)$ and $c = 12.996(3)$ Å; spinel, $a = 8.085(1)$ Å; and forsterite, $a = 4.756(1)$, $b = 10.200(1)$, and $c = 5.981(1)$ Å.

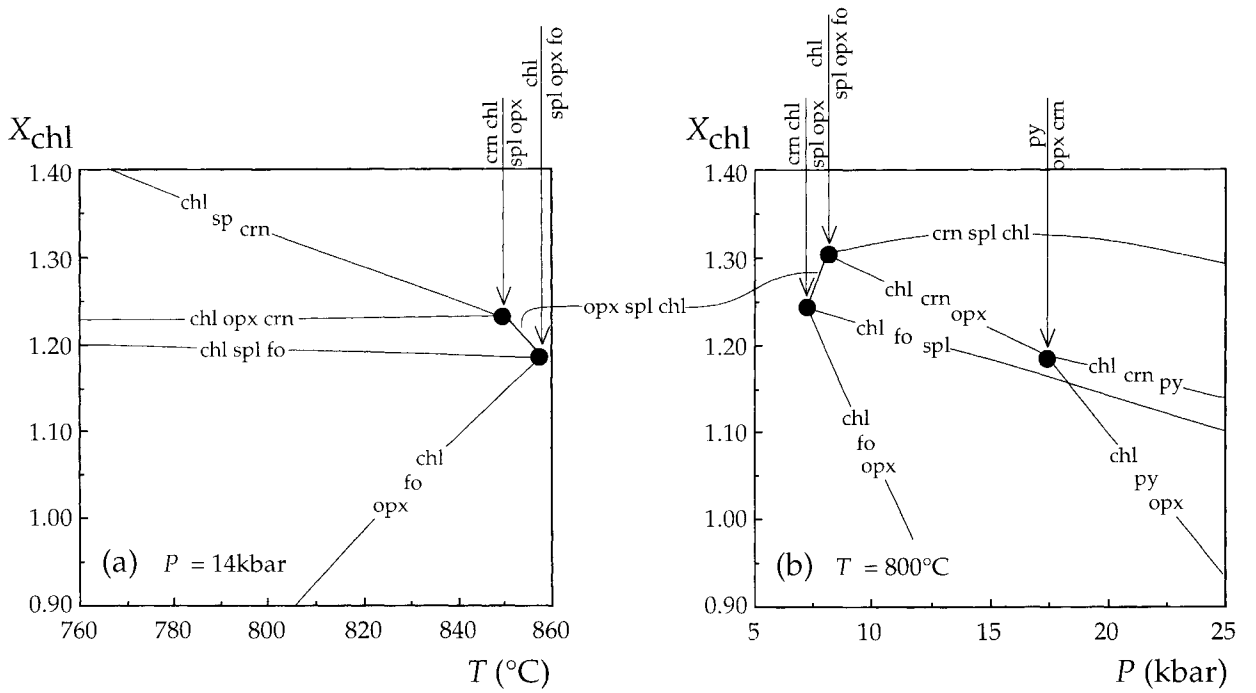

FIGURE 3. The variation of X_{chl} in divariant assemblages at **(a)** $P = 14$ kbar and **(b)** $T = 800$ °C, calculated using the simple a-X model of Holland and Powell (1990). Mineral abbreviations as in Figure 1. Solid circles show the conditions at which univariant reactions take place; the reaction taking place in each case is given on the adjacent arrow.

Experimental procedure

The compositions of chlorite in two divariant assemblages (chlorite + orthopyroxene + forsterite and chlorite + corundum + spinel) were investigated experimentally. Individual experiments contained two 1.5 mm diameter platinum capsules; both capsules contained the same divariant assemblage, but the mix in each capsule included only one of the two starting chlorite samples (experiments labeled "a" contained chlorite a, $X_{chl} = 1.37$–1.44, and those labeled "b" contained chlorite b, $X_{chl} = 0.97$). Both mixes in each experimental pair were identical in bulk composition; experiments involving chlorite + orthopyroxene + forsterite had a bulk composition equivalent to a chlorite of composition $X_{chl} = 0.82$, and those involving chlorite + corundum + spinel had a bulk composition equivalent to a chlorite of composition $X_{chl} = 1.67$. In addition to 8 mg of mix, each platinum capsule contained 6 mg of deionized water.

Successful experiments showed no weight gain or loss after the experiment and produced water when the capsule was pierced (i.e., water was still present in excess). The experimental products were examined optically and with X-ray diffraction to confirm that all phases in the divariant assemblage were still present and that no other phases had grown during the experiment. Individual chlorite X-ray reflections were well defined and showed no asymmetry, suggesting almost complete reequilibration of the chlorite and the absence of compositional zonation.

TABLE 1. Compositions and synthesis conditions of phases used in this study

Phase	Composition	T (°C)	P	t (h)
Chlorite a*	$Mg_{4.56-4.63}Al_{2.88-2.74}Si_{2.56-2.63}O_{10}(OH)_8$	580–650	15 kbar	65
Chlorite b*	$Mg_{5.03}Al_{1.94}Si_{3.03}O_{10}(OH)_8$	620–700	15 kbar	65
Chlorite c*	$Mg_{5.17}Al_{1.66}Si_{3.17}O_{10}(OH)_8$	620–700	15 kbar	65
Orthopyroxene*	$Mg_{1.89}Al_{0.22}Si_{1.89}O_6$	910	7 kbar	18
Spinel	$MgAl_2O_4$	1350	1 atm	264
Corundum	Al_2O_3	1350	1 atm	48
Forsterite	Mg_2SiO_4	800	1.5 kbar	216

* Analyzed using electron microprobe; see text.

TABLE 2. Unit-cell parameters of synthetic chlorite used in this study

Sample	X_{chl}*	a (Å)	b (Å)	c (Å)	V (Å³)
			Chlorite a		
50	1.37	5.311(1)	9.198(1)	14.288(3)	692.53(15)
53	1.39	5.313(2)	9.199(2)	14.292(4)	693.08(23)
55**	1.44	5.310(1)	9.195(1)	14.283(3)	691.92(18)
			Chlorite b		
25	0.97	5.322 (1)	9.217(1)	14.396(3)	700.70(18)
26	0.97	5.324 (1)	9.218(1)	14.395(3)	701.06(14)
mdw	0.97	5.322 (1)	9.216(1)	14.401(3)	700.97(17)
			Chlorite c		
59	0.83	5.323(2)	9.220(2)	14.445(4)	703.43(22)

Note: The values in parentheses are 1σ errors in the last digit(s).
* X_{chl} is defined in the text.
** XRD trace showed traces of spl + crn (<5%).

TABLE 3. Peak positions and *hkl* indices used for refinements of chlorite unit-cell parameters in this study

hkl	Chlorite a	Chlorite b	Chlorite c
004	25.070	24.904	24.828
005	31.510	31.278	31.172
$\bar{2}01$	33.776	33.710	33.730
$20\bar{2}$	34.771	34.684	34.692
201	35.364	35.275	35.274
$20\bar{3}$	36.888	36.777	36.776
202	37.841	37.709	37.690
$20\bar{4}$	39.979	39.825	39.780
$20\bar{5}$	43.851	43.668	
007	44.710	44.356	
204	45.323	45.096	45.048
$20\bar{6}$	48.380	48.144	48.044
205	50.029	49.776	49.685
$20\bar{8}$	59.039	58.673	58.514
060	60.315	60.176	60.178
062	61.878	61.714	61.691
063	63.776	63.591	63.536
064	66.356	66.174	66.099
208	67.137	66.706	66.544
065	69.674	69.396	
066	73.562	73.253	73.179

RESULTS AND DISCUSSION

Unit-cell calibration

It is well established in the literature that chlorite unit-cell parameters vary linearly with chlorite composition, but studies by Nelson and Roy (1958), Shirozu and Momoi (1972), Jenkins and Chernosky (1986), McPhail et al. (1990), and, most recently, Roots (1994) all produced different calibrations. The compositions of the chlorite in all these studies were, however, determined indirectly; chlorite samples were synthesized from oxide mixes or gels, and, after careful optical and SEM examination to ensure that other mineral phases were not present, it was assumed that the synthetic chlorite samples were "on composition." In this study, the compositions of the synthetic chlorite used in the calibration were determined using the SX-50 electron microprobe at the University of Cambridge. Specimens were prepared as grain mounts in epoxy, and compositions of individual chlorite grains were analyzed with beam currents of 5 nA and an accelerating voltage of 10 kV. Because of the fine grain size and porous nature of the synthetic materials, oxide weight-percent totals ranged from 70 to 85%. The composition of individual chlorite analyses from a particular sample were determined by normalizing the analyzed oxide total to the theoretical total (87.05% for chlorite a, 87.04% for chlorite b, and 87.03% for chlorite c). The chemical formulas derived from these analyses were independent of the original analytical total, indicating that these low totals did not result in differential loss of Mg, Al, or Si. Averages of the chemical formulas derived from all the analyses of a particular sample were then used to calculate the value of X_{chl} from the Al, Si, and Mg atoms pfu (i.e., $X_{chl} = 6 - Mg = 0.5Al = 4 - Si$), and the average of these three values was taken as the composition of the synthetic chlorite sample. These compositions are given in Table 2.

The compositions of the synthetic chlorite were ostensibly 1.50, 1.00, and 0.75 (chlorite samples a, b, and c, respectively) on the basis of the composition of the oxide mix from which each was synthesized. However, electron microprobe analysis of the composition of chlorite c ($X_{chl} = 0.83$) indicated that it is more aluminous than the original oxide mix ($X_{chl} = 0.75$). This is the result of the growth of the Al-poor phases orthopyroxene and forsterite. The composition of chlorite b is similar to that of the starting oxide mix, and this is consistent with the apparently monomineralic nature of the synthesis products. However, a significant departure from the composition of the original oxide mix was observed in the Al-rich syntheses. Although one of these syntheses was observed to contain small amounts of spinel and corundum, these phases were not observed either optically or with SEM in the other two syntheses. However, microprobe analyses of all three syntheses showed similar compositions ($X_{chl} \approx 1.4$), significantly less aluminous than the nominal composition of $X_{chl} = 1.5$. Thus, all three syntheses must contain aluminous phases in addition to chlorite, but only in one synthesis did these phases grow to a sufficient size to be observed using XRD. This result indicates the importance of analyzing the compositions of chlorite used in developing a calibration of unit-cell parameters.

Eighteen to 21 reflections with 2θ angles between 20 and 75° were used for the least-squares refinement of the unit-cell parameters of the synthetic chlorite. These reflections are listed in Table 3, and the refined unit-cell parameters for the synthetic chlorite are given in Table 2. Figure 4 shows the variation in the unit-cell parameters (*a, b, c, V,* and β) with composition of the chlorite. The results of previous studies are also shown for reference.

From Figure 4, it can be seen that the variation in the unit-cell parameters of all the available data for chlorite is, indeed, a linear function of the composition of the chlorite. However, there is a considerable spread in the

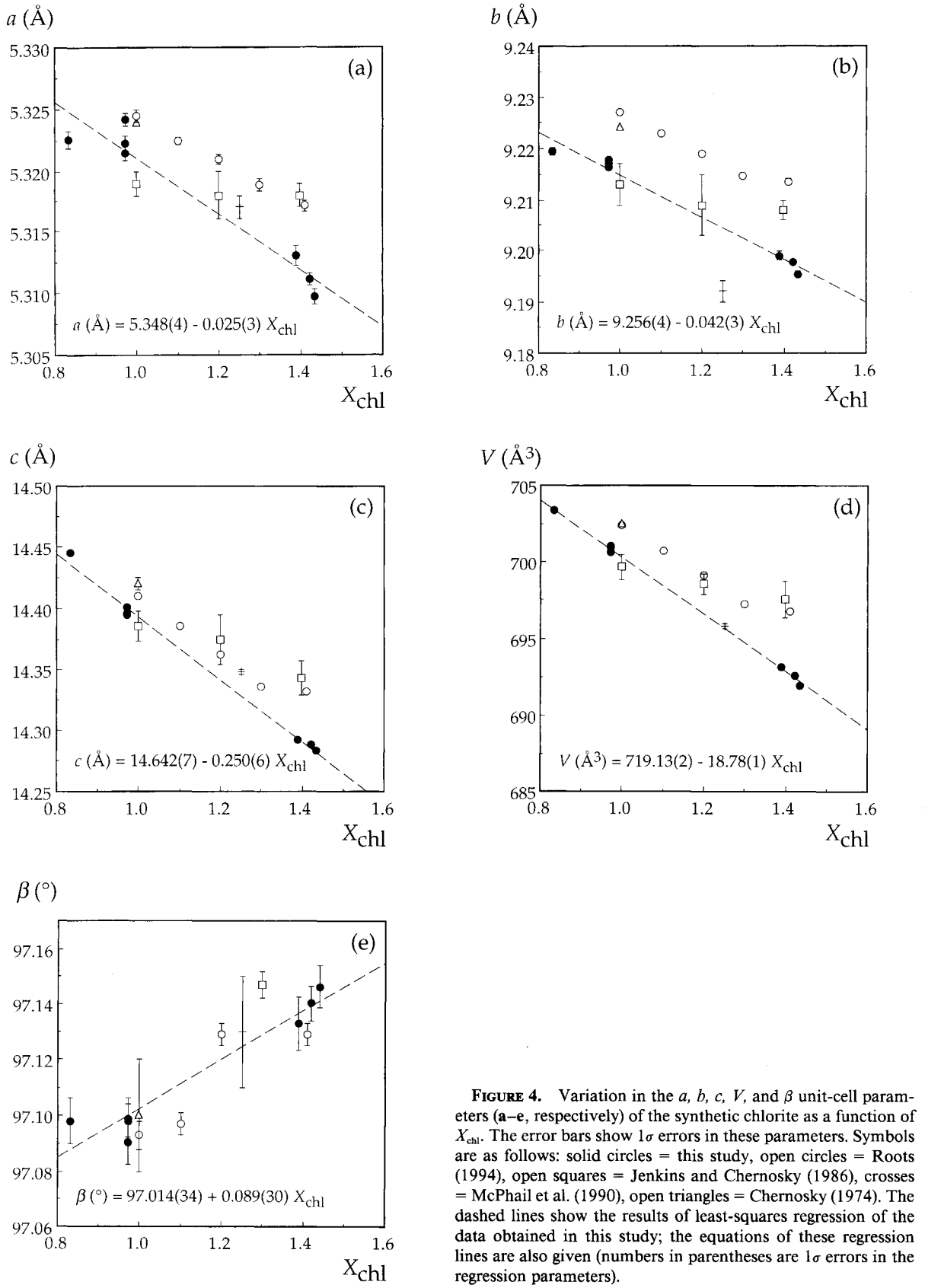

Figure 4. Variation in the *a*, *b*, *c*, *V*, and β unit-cell parameters (**a**–**e**, respectively) of the synthetic chlorite as a function of X_{chl}. The error bars show 1σ errors in these parameters. Symbols are as follows: solid circles = this study, open circles = Roots (1994), open squares = Jenkins and Chernosky (1986), crosses = McPhail et al. (1990), open triangles = Chernosky (1974). The dashed lines show the results of least-squares regression of the data obtained in this study; the equations of these regression lines are also given (numbers in parentheses are 1σ errors in the regression parameters).

TABLE 4. Compositions and unit-cell parameters of chlorite from experimental reversals

Expt.*	P (kbar)	T (°C)	t (h)	c (Å)	X_{chl}**
		Chlorite + orthopyroxene + forsterite			
60a	14	840	118	14.369(2)	1.09
60b	14	840	118	14.371(2)	1.08
62a	14	820	141	14.373(2)	1.07
63a	14	800	141	14.384(3)	1.03
63b	14	800	141	14.386(3)	1.03
67a	14	780	236	14.396(1)	0.99
67b	14	780	236	14.396(1)	0.98
65a	18	800	119	14.387(1)	1.02
65b	18	800	119	14.391(2)	1.00
64a	16	800	166	14.380(2)	1.05
64b	16	800	166	14.391(1)	1.01
66a	12	800	187	14.374(1)	1.07
66b	12	800	187	14.381(1)	1.04
68a	10	800	260	14.370(1)	1.09
68b	10	800	260	14.375(2)	1.07
		Chlorite + corundum + spinel			
75a	14	820	119	14.353(1)	1.16
75b	14	820	119	14.359(1)	1.13
76a	14	800	144	14.342(2)	1.20
76b	14	800	144	14.352(2)	1.16
80a	14	780	192	14.340(2)	1.21
80b	14	780	192	14.342(2)	1.20
78a	17.9	800	119	14.332(1)	1.24
79a	16	800	139	14.335(2)	1.23
79b	16	800	139	14.334(2)	1.23
77a	11.9	800	115	14.343(1)	1.20
77b	11.9	800	115	14.344(2)	1.19

Note: The values in parentheses are 1σ errors in the last digit(s).

* Experiments labeled "a" started with chlorite a, experiments labeled "b" started with chlorite b.

** The values of X_{chl} were calculated using the c-X_{chl} calibration presented in the text.

data for any particular parameter, with the data from this study typically falling to one side of the published data. Given the departure of the actual composition from the nominal composition observed in the synthetic chlorite samples in this study, it is possible that the spread of the data is, at least in part, due to trace amounts of aluminous phases not detected during examination of the synthetic materials. This material, if present, would coexist with a chlorite of lower X_{chl} (i.e., Al content) than the original mix, and correction for this compositional error would translate the data toward that obtained in the present study. Because of the possibility of compositional errors, the data from previous studies were excluded from the fitting; the linear least-squares regression of the data presented in this study gives the following calibrations: a (Å) = 5.348(4) − 0.025(3)X_{chl}, b (Å) = 9.256(4) − 0.042(3)X_{chl}, c (Å) = 14.642(7) − 0.250(6)X_{chl}, V (Å^3) = 719.13(2) − 18.78(1)X_{chl}, and β (°) = 97.014(34) + 0.089(30)X_{chl}. In addition to providing a means of determining the composition of MASH chlorite from the unit-cell parameters, these new measurements allow improved estimates of the molar volumes for clinochlore (210.88 cm^3/mol) and amesite (205.53 cm^3/mol) end-members. The clinochlore volume is within error of that used (210.90) by Holland and Powell (1990), but the new amesite volume is considerably smaller than their tabulated value of 209.80 cm^3/mol, which was based on the data of Jenkins and Chernosky (1986).

Experimental reversals

The composition of chlorite in each experiment was determined from the lattice parameters using the calibration derived above of variation in the c lattice parameter with composition. The lattice parameters and the corresponding composition of the chlorite for each experiment are given in Table 4.

The bracketed compositions of the chlorite and the results of the calculations using the Holland and Powell dataset (generated January 26, 1995) and the simple a-X model for chlorite are compared in Figure 5 (curve 1). Three important discrepancies are observed. First, at 14 kbar, the calculated composition of chlorite at the breakdown reaction is too aluminous in comparison with the composition bracketed by the experimental results. Second, the calculated slopes for the divariant assemblage chlorite + orthopyroxene + forsterite, dX/dT and dX/dP, are significantly steeper than the experimental data. Finally, although the calculations for the chlorite + corundum + spinel divariant assemblage appear to have the correct slope in P-T-X_{chl} space, the calculated chlorite compositions are too aluminous. The possible reasons for the discrepancies between the results of calculations and the experimental data are discussed below.

The discrepancies between the calculated and observed Al contents of chlorite at the breakdown temperature result, in part, because Holland and Powell (1990) used the calibration of Jenkins and Chernosky (1986) in their derivation of thermodynamic data for chlorite. Figure 6 compares the experiments of Jenkins and Chernosky (1986) and the results presented above. Although the bracketed compositions of chlorite in this study show a more rapid increase in the c unit-cell parameter with decreasing temperature than the unreversed synthesis experiments presented in Jenkins and Chernosky (1986), the results of both studies indicate a similar c unit-cell parameter (i.e., X_{chl}) for chlorite at its breakdown to forsterite + orthopyroxene + spinel. However, the chlorite composition to which this value of c corresponds depends on which of the c-X_{chl} calibrations is adopted. Using the c-X_{chl} calibration presented in Jenkins and Chernosky (1986), the composition of chlorite at its breakdown at 14 kbar is X_{chl} = 1.2; using the calibration derived in this study, the composition is X_{chl} = 1.1. To make the calculations using clinochlore consistent with the new experimental value of X_{chl} = 1.1 at the conditions of the breakdown of chlorite to orthopyroxene + forsterite + spinel + H_2O (14 kbar and 850 °C), the enthalpies of formation for clinochlore and amesite were rederived, and the results of calculations using these revised values and the new molar volumes for amesite and clinochlore are shown in Figure 5 (curve 2). Comparison with the original data shows that this correction has simply moved the entire set of curves to higher values, removing the discrepancy between the calculated and experimentally determined

compositions of chlorite at its breakdown in Figure 5 and improving the match between the experimental and calculated compositions of chlorite in the divariant chlorite + corundum + spinel assemblage. However, the calculations still fail to match the slopes and positions of the experimentally determined divariant assemblage chlorite + orthopyroxene + forsterite.

In the calculations above, compositions were allowed to vary only for the orthopyroxene and chlorite phases. Thus, one explanation for the discrepancy between the calculated and experimental results for the chlorite + orthopyroxene + forsterite divariant assemblages is that the composition of the orthopyroxene (the Al content) did not reequilibrate in the experiments. The effect of differences in the Al content of the orthopyroxene on the model calculations can be tested by fixing the composition of the orthopyroxene at $X_{en} = 0.89$ (i.e., the starting material) and recalculating the change in the composition of the chlorite with pressure and temperature. Across the P-T range of interest, the maximum differences in the recalculated compositions of the chlorite are $X_{chl} = 0.05$ at 780 °C and 14 kbar and $X_{chl} = 0.04$ at 800 °C and 18 kbar, and these differences decrease with increasing temperature and decreasing pressure. The differences between the calculated and experimental compositions of $X_{chl} = 0.36$ at 780 °C and 14 kbar and $X_{chl} = 0.41$ at 800 °C and 18 kbar make it clear that variations in the Al content of the orthopyroxene cannot be the sole cause of the observed discrepancies in the case of the chlorite + orthopyroxene + forsterite divariant assemblage.

We therefore consider that the probable reason for the discrepant slopes lies in the nature of the a-X model used for chlorite solid solutions, and we thus investigated a variety of different activity-composition relations for this type of charge-balanced Tschermak substitution to improve the fit of the calculations to the experiments. Interestingly, it is the simplest of these models (an effective one-site, or molecular, solution of clinochlore and amesite) that comes closest to fitting the experimental reversals. In this model the activities are given by $a_{clin} = 2 - X_{chl}$ and $a_{ames} = X_{chl} - 1$, with X_{chl} ranging between 1 (clinochlore) and 2 (amesite). The resulting calculations, calibrated on $X_{chl} = 1.1$ at the chlorite breakdown, are shown in Figure 5 (curve 3). Although the agreement with

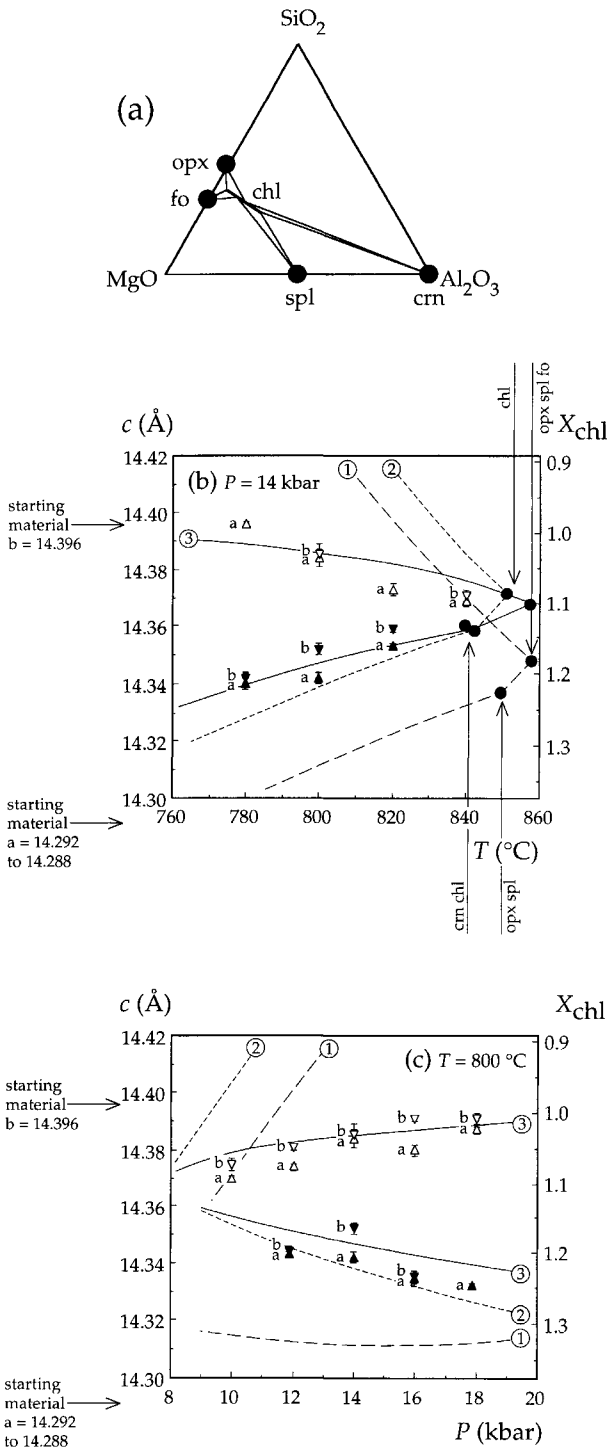

FIGURE 5. (a) A schematic MgO-Al_2O_3-SiO_2 compatibility triangle showing the stable tie lines between chlorite, corundum, orthopyroxene, forsterite, and spinel at $P = 14$ kbar. Mineral abbreviations as in Figure 1. (b and c) The c unit-cell parameters (error bars show 1σ errors) of chlorite from the experimental reversal experiments for the divariant assemblages chlorite + orthopyroxene + forsterite (open triangles) and chlorite + spinel + corundum (solid triangles) are shown in b for $P = 14$ kbar and c for $T = 800$ °C. The lattice parameters of the starting chlorite samples (i.e., samples a and b) are indicated; individual experimental half-brackets are labeled "a" or "b" to indicate the chlorite used. Curves 1, 2, and 3 in b and c show the results of theoretical calculations; these are discussed in detail in the text and were superimposed on the experimental data using the c-X_{chl} calibration derived in this study. Solid circles show the P-T conditions of univariant reactions; the reaction taking place in each case is given on the adjacent arrow.

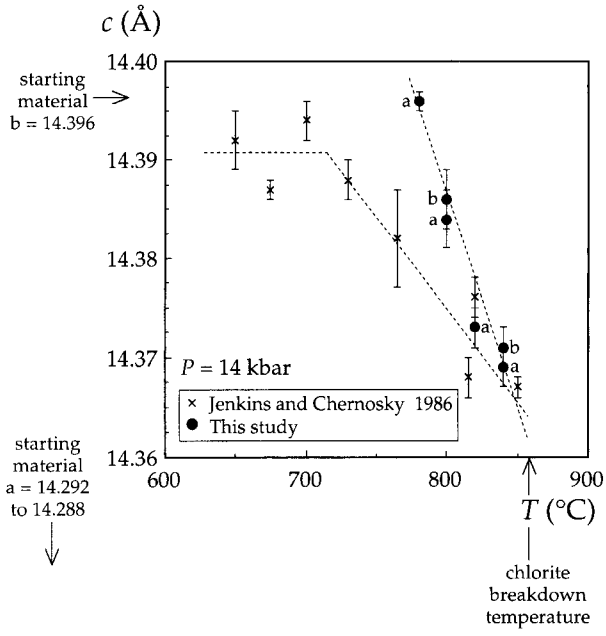

FIGURE 6. Variation in the c unit-cell parameter of chlorite coexisting with forsterite and orthopyroxene at $P = 14$ kbar. The error bars show 1σ errors in the measurements. Individual experimental half-brackets from this study are labeled "a" or "b" to indicate the chlorite used.

the experiments is reasonable, this is not an endorsement of the one-site solution because the model does not allow variation of chlorite compositions to lower Al contents than clinochlore ($X_{chl} = 1.0$), and Al-poor chlorite is known to occur in both natural assemblages and in experimental studies such as this one. However, the apparent success of the one-site model provides strong supportive evidence that entropies of mixing are very low in chlorite solid solutions, far lower than in any of the ideal mixing-on-sites models so far proposed. A new model that preserves this low entropy and allows for solid solution from amesite through to the serpentine composition will be introduced and calibrated, and its geological implications explored, in another study (Holland et al., in preparation). It remains likely, however, that the simple one-site model, although conceptually flawed, will furnish a useful approximation for calculations involving chlorite as long as the compositions of interest are more aluminous than clinochlore.

ACKNOWLEDGMENTS

This research was supported by NERC grant GR9/00974 (to J.B. and T.J.B.H.) and NERC grant GR9/1285 and Royal Society grant 574005.G501/JECL/SM (both to D.C. Palmer, University of Cambridge). Mark Welch is thanked for discussion and assistance with experimental procedures and orthopyroxene and gel preparation, and Brian Cullum is thanked for his assistance in the laboratory. We are also grateful to S. Reed for his assistance with microprobe analysis of very fine-grained samples.

REFERENCES CITED

Berman, R.G. (1988) Internally-consistent thermodynamic data for minerals in the system, Na_2O-K_2O-CaO-MgO-FeO-Fe_2O_3-Al_2O_3-SiO_2-TiO_2-H_2O-CO_2. Journal of Petrology, 29, 445–522.

Brown, B.E., and Bailey, S.W. (1962) Chlorite polytypism: I. Regular and semirandom one-layer structures. American Mineralogist, 47, 819–850.

Chernosky, J.V., Jr. (1974) The upper stability of clinochlore at low pressure and the free energy of formation of Mg-cordierite. American Mineralogist, 59, 496–507.

Chernosky, J.V., Berman, R.G., and Bryndizia, L.T. (1988) Stability, phase relations and thermodynamic properties of chlorite and serpentine group minerals. In Mineralogical Society of America Reviews in Mineralogy, 19, 295–346.

Danckwerth, P.A., and Newton, R.C. (1978) Experimental determination of the spinel peridotite to garnet peridotite reaction in the system MgO-Al_2O_3-SiO_2 in the range 900 °C–1000 °C and Al_2O_3 isopleths of enstatite in the spinel field. Contributions to Mineralogy and Petrology, 66, 189–201.

Fawcett, J.J., and Yoder, H.S., Jr. (1966) Phase relations of chlorites in the system MgO-Al_2O_3-SiO_2-H_2O at 2 kbar water pressure. American Mineralogist, 51, 353–380.

Gasparik, T., and Newton, R.C. (1984) The reversed alumina constants of orthopyroxene in equilibrium with spinel and forsterite in the system MgO-Al_2O_3-SiO_2. Contributions to Mineralogy and Petrology, 85, 186–196.

Hamilton, D.L., and Henderson, C.M.B. (1968) The preparation of silicate compositions by a gelling method. Mineralogical Magazine, 36, 832–838.

Hays, J.F., and Bell, P.M. (1973) Albite-jadeite-quartz equilibrium. Carnegie Institution of Washington Year Book, 72, 706–708.

Holland, T.J.B., and Powell, R. (1990) An internally consistent thermodynamic dataset with uncertainties and correlations: The system Na_2O-K_2O-CaO-MgO-MnO-FeO-Fe_2O_3-Al_2O_3-SiO_2-TiO_2-C-H_2-O_2. Journal of Metamorphic Geology, 8, 89–124.

Jenkins, D.M. (1981) Experimental phase relations of hydrous peridotites modelled in the system H_2O-CaO-MgO-Al_2O_3-SiO_2. Contributions to Mineralogy and Petrology, 77, 166–176.

Jenkins, D.M., and Chernosky, J.V., Jr. (1986) Phase equilibria and crystallochemical properties of Mg-chlorite. American Mineralogist, 71, 924–936.

McPhail, D., Berman, R.G., and Greenwood, H.J. (1990) Experimental and theoretical constraints on aluminum substitution in magnesian chlorite, and a thermodynamic model for H_2O in magnesian cordierite. Canadian Mineralogist, 28, 859–874.

Nelson, B.W., and Roy, R. (1958) Synthesis of the chlorites and their structural and chemical constitution. American Mineralogist, 43, 707–725.

Powell, R., and Holland, T.J.B. (1988) An internally consistent thermodynamic dataset with uncertainties and correlations: 3. Application methods, worked examples and a computer program. Journal of Metamorphic Geology, 6, 173–204.

Roots, M. (1994) Molar volumes on the clinochlore-amesite binary: Some new data. European Journal of Mineralogy, 6, 279–283.

Shirozu, H., and Momoi, H. (1972) Synthetic Mg-chlorite in relation to natural chlorite. Mineralogical Journal, 11, 161–171.

Staudigel, H., and Schreyer, W. (1977) The upper thermal stability of clinochlore, $Mg_5Al[Si_3Al]O_{10}(OH)_8$, at 10–35 kbar $P(H_2O)$. Contributions to Mineralogy and Petrology, 61, 187–198.

Welch, M.D., Barras, J., and Klinowski, J. (1995) A multinuclear NMR study of clinochlore. American Mineralogist, 80, 441–447.

MANUSCRIPT RECEIVED JUNE 27, 1995
MANUSCRIPT ACCEPTED JANUARY 12, 1996